



Analysis of Love-type surface waves in an isotropic thermoelastic layer over a non-homogeneous elastic half-space with interface irregularity

Suraj Sharma, Ravinder Kumar*

Department of Mathematics, University Institute of Sciences, Chandigarh University, Mohali-140413, Punjab, India

Abstract

This study explores the dispersion characteristics of Love-type surface waves in a composite elastic media consisting of an isotropic thermoelastic layer resting over nonhomogeneous elastic half-space. A rectangular-shaped irregularity at the interface between the two media is introduced to simulate a geometric discontinuity, which represents more realistic subsurface features. The present work simultaneously incorporates material inhomogeneity, thermoelastic effects, and interface irregularity within a unified analytical framework. The governing equations have been taken using theory of elasticity and solved analytically using Fourier and inverse Fourier transformations. Perturbation method is then applied to derive the dispersion equation for the propagation of Love waves. This dispersion equation is graphically analysed using MATLAB to observe how the dimensionless phase velocity changes with dimensionless wave number for different values of the inhomogeneity parameter and various values of the ratio of irregularity depth to layer height. The obtained results show that both rectangular-shaped interface irregularity and inhomogeneity significantly affect phase velocity, particularly at the lower wave numbers. This study enhances the understanding of surface wave behaviour in complex elastic structures and provides practical implications for subsurface imaging, seismic hazard assessment, and material characterization in civil engineering and geotechnical applications.

DOI:10.46481/jnsps.2026.3231

Keywords: Love waves, Interface irregularity, Thermoelastic layer, Dispersion equation, Nonhomogeneous half-space

Article History :

Received: 29 November 2025

Received in revised form: 09 February 2026

Accepted for publication: 18 February 2026

Published: 21 March 2026

© 2026 The Author(s). Published by the [Nigerian Society of Physical Sciences](#) under the terms of the [Creative Commons Attribution 4.0 International license](#). Further distribution of this work must maintain attribution to the author(s) and the published article's title, journal citation, and DOI.

Communicated by: B. J. Falaye

1. Introduction

Seismology is a branch of science that studies the elastic waves produced by natural events like earthquakes and volcanic eruptions, and also by human activities such as explosions. The study of these waves, help scientists to understand the structure of the Earth, track movements of tectonic plates, and to evaluate the areas at risk of earthquakes. The major focus of seismology is earthquakes, which occur when built-up stress along

fault lines is suddenly released. The released energy propagates in all directions through the Earth in the form of elastic disturbances that provide valuable information about subsurface features. The foundational insights into seismology, and associated phenomena can be found in the works of Shearer [1], Gubbins [2], and Biot [3]. Seismic waves are generally classified into body waves and surface waves where the body waves travel in the interior of Earth whereas the surface waves travel along the surface of Earth. Among the surface waves, Love waves have received specific attention due to their abil-

*Corresponding author Tel. No: +91-989-611-1779.

ity to concentrate energy near the Earth's surface. This highly sensitive nature makes them effective for detecting changes in subsurface material properties, layer thickness, and irregularities at the interface. Love waves are shear-horizontal waves that travels in a stratified medium and their purely horizontal particle motion simplifies the mathematical treatment and makes them very useful for the subsurface imaging, and seismic hazard assessment. Classical studies on the propagation of Love waves often used the simplifying assumption of isotropic and homogeneous elastic media. However, such assumptions not always succeed to represent real geological environments conditions, where materials possess inhomogeneity, thermoelastic coupling, and surface irregularities. Thermoelasticity describes the relationship between the mechanical and thermal fields, becomes significant in environments where thermal changes affect material behaviour. Similarly, spatial changes in elastic moduli and density within the inhomogeneous media presents attenuation and dispersive behaviour that affects wave characteristics.

The fundamental work on Love waves began with Love [4], who presents the shear horizontal wave motion in an isotropic, homogeneous elastic layer over a semi-infinite half-space. After this, further studies have investigated the impact of multi-layered geometries, viscoelasticity, anisotropy, and more complex structures. Ewing *et al.* [5] studied how layer thickness and rigidity effect on the dynamics of surface wave. Graff [6] showed the dependence of frequency on dispersion relations for surface waves, while Achenbach [7] investigated the surface wave propagation in layered elastic media. Chattopadhyay and Kar [8] used the Green's function methods to examine Love wave propagation behaviour under initial stress conditions. These basic studies provide theoretical understanding, but most of the studies were confined to ideal conditions of homogeneity and isotropy. Studying wave propagation through nonhomogeneous media, where material properties change with respect to position, is important for modelling real-world physical systems. One significant characteristic of these media is that spatial variations have an impact on wave propagation. Kundu *et al.* [9] explored the heterogeneity and micropolar effects on Love waves in multi-layered media. Kumar and Saini [10] used theory of elasticity to study Love wave propagation in a fluid-saturated porous layer bounded by a homogeneous layer and a nonhomogeneous half-space and showed the effect of porosity, anisotropy, and inhomogeneity on phase velocity. Chattopadhyay *et al.* [11] studied the effect of inhomogeneity on phase velocity of Love waves in isotropic tri-layers system.

The theory of thermoelasticity has changed significantly over the years, starting with Biot [12] and Nowacki [13], who developed the initial models coupling thermal effects and mechanical fields through irreversible thermodynamics. These models were later generalized by Dhaliwal and Singh [14] to analyse both transient and steady-state responses under thermal effects. Lord and Shulman [15] proposed a generalized thermoelasticity theory, that incorporated a hyperbolic type equation of heat conduction with a relaxation time. Such a model was improved by Green and Lindsay [16] by adding two relaxation times to the model to describe thermoelastic interactions over a wider range of conditions. Green and Naghdi [17]

further advanced this theory by formulating generalized thermoelasticity, that allowed for undamped thermal waves. Later discoveries, including the Dual Phase Lag theory by Tzou [18], give a unified structure in which not only temperature gradients but also heat fluxes delay in time. Sharma *et al.* [19] studied how thermoelastic waves travel through homogeneous isotropic plates under various thermal conditions using multiple generalized thermoelasticity. Berezovski *et al.* [20] introduced a thermodynamically consistent approach for modelling thermoelastic waves in inhomogeneous media, addressing limitations in traditional continuum-based methods. Since then, many studies have investigated thermoelastic effects in multi-layered systems, showing significant effects in phase velocity due to thermal relaxation. Chirita [21] conducted a comprehensive analysis on how Rayleigh surface waves move through anisotropic, homogeneous thermoelastic half-spaces by incorporating thermal dissipative effects into the elastic wave model. Pramanik and Biswas [22] proposed a comprehensive theoretical model to investigate the behaviour of Rayleigh surface waves in a nonlocal thermoelastic medium using nonlocal elasticity theory combined with thermoelasticity and energy dissipation principles. Kumar *et al.* [23] studied Love waves in a thermoelastic layer and observed how thermal stresses impact wave dispersion, providing a direct link between temperature variations and wave behaviour.

The Earth's crust is uneven, containing different kinds of irregularities at the interface that form naturally or due to underground explosions. These interface irregularities have a great influence on the seismic wave propagation by changing their dispersion characteristics. Consequently, the existence of these irregularities at the interface complicates the propagation of surface waves that are significant in earthquake study as well as in testing materials. The study of these effects has been one of the main concerns for the seismologists and researchers who have formulated different models and methodologies in which the irregularities, including other aspects that affect the seismic wave propagation are taken into account. Madan *et al.* [24] extended the theoretical framework established by Konczak [25] by examining the influence of interface irregularity and rigidity conditions on the propagation characteristics of Love waves in a fluid-saturated porous layer. In their study, they considered a model where a rectangular-shaped interface irregularity exists between the layer and the half space. Kumar *et al.* [26, 27] investigated the effect of triangular-shaped irregularity and inhomogeneity on shear wave propagation in an anisotropic porous layer. Sharma and Kumar [28] conducted a theoretical investigation into the propagation behaviour of shear waves in an anisotropic porous layer. The paper analyzed the effect of porosity and initial stress on the phase velocity. Saini and Kumar [29, 30] examined the interaction effects of porosity, parabolic-shaped interface irregularity and initial stress in multilayered media, highlighting how these factors can influence the Love waves dispersion equation in an anisotropic porous layer over a heterogeneous half-space. Kumar and Saini [31] studied the Love-wave behaviour in a porous layer that placed between a homogeneous isotropic layer and an elastically nonhomogeneous half-space, whereby the interface has a

parabolic-shaped irregularity. Sharma and Kumar [32] analysed Love-wave propagation in an isotropic thermoelastic layer and investigated the combined influence of thermoelastic effects, inhomogeneity and irregularity on the phase velocity and the behaviour of waves. Other contributions to this area have been done by Pragati *et al.* [33], Thakur *et al.* [34] and Saini and Kumar [35]. The literature review shows that there has been a significant progress in our understanding of Love-wave behaviour in a range of complex systems. However, existing literature often separates individual effects, like thermoelasticity, inhomogeneity, or geometric irregularities, rather than examining their combined effects. This study aims to bridge the gap by formulating a comprehensive model that consider these complexities, providing a more realistic representation of behaviour of Love wave propagation in layered systems.

This study focuses on exploration into the behavior of Love waves that travel in an isotropic thermoelastic layer that has a free upper surface and is placed over a nonhomogeneous half-space. This study incorporates a triangular-shaped irregular boundary condition, offering a more realistic scenario for propagation of surface wave. The fundamental equations are obtained within the framework of the theory of elasticity, and the use of Fourier transforms. Perturbation method is then applied to find the dispersion relation. The resulting algebraic equation is solved to determine the effect of inhomogeneity of the material, and geometrical irregularity on the phase velocity. The findings of this investigation are quite relevant to seismic hazard modelling, geophysical exploration, and design of layered structures that are vulnerable to thermal stresses.

2. Formulation of the problem

This research considers a composite structure consisting of a thermoelastic layer of thickness H with upper free surface, resting on a nonhomogeneous half-space. At the interface of these two mediums, a rectangular-shaped irregularity is considered, with a height of h and width of $2s$. This geometry is described using a 3D Cartesian coordinate (x, y, z) (Figure 1), where the origin is pointed at the centre point of the rectangular-shaped interface irregularity. In this setup, the z -axis is pointing vertically downward, and the x -axis which is perpendicular to it lies horizontally along the plane of half-space. The source of the disturbance that generated the interface irregularity is located at the $(0, 0, d)$ point on the positive z -axis with $d > h$. According to this arrangement, model is divided into two distinct parts:

- The first medium, denoted as M_1 corresponds to upper thermoelastic layer and spans $-H \leq z < 0$
- The second medium, denoted as M_2 represents the elastic, nonhomogeneous half-space and spans $0 \leq z < \infty$

The equation for the irregular interface is represented as $z = \varepsilon f(x)$.

For a rectangular-shaped irregularity, the surface profile can be represented as

$$f(x) = \begin{cases} 2s; & -s < x < s \\ 0; & x > s, x < -s, \end{cases} \quad (1)$$

where $\varepsilon = h/2s \ll 1$ and $s \neq 0$.

3. Governing equations and constitutive relations

To analyse the propagation of Love waves in the given structure, it is necessary to define the governing equations along with the constitutive relations for both mediums. The formulation uses the generalized thermoelastic theory for the first medium M_1 and elasticity theory for the second medium M_2 taking into account temperature effects as well as changes in material properties.

According to Lord and Shulman [15], the fundamental governing equations describing the behaviour of the medium M_1 in the absence of external heat sources and body forces, can be expressed as follows

$$\mu_1 \nabla^2 \mathbf{v} + (\lambda_1 + \mu_1) \nabla(\nabla \cdot \mathbf{v}) - \beta \nabla \theta = \rho_1 \ddot{\mathbf{v}}, \quad (2)$$

$$K \nabla^2 \theta - \beta T_0 \nabla \cdot \dot{\mathbf{v}} - a T_0 \dot{\theta} = 0, \quad (3)$$

where v denotes the displacement component, $\beta = (3\lambda_1 + 2\mu_1)\alpha$ is the thermoelastic coupling parameter and α denotes the coefficient of linear thermal expansion, ρ_1 is mass density of the thermoelastic layer, θ represents the temperature change from the reference temperature T_0 , μ_1 and λ_1 are Lamé's elastic constants, K is thermal conductivity, and the superposed dot denotes differentiation with respect to time.

The constitutive relations for medium M_1 are given as

$$t_{ij} = \lambda_1 e_{kk} \delta_{ij} + 2\mu_1 e_{ij} - \beta \theta \delta_{ij}, \quad (4)$$

where

$$e_{kk} = v_{kk}, \quad 2e_{ij} = v_{i,j} + v_{j,i}. \quad (5)$$

This study considers a two-dimensional problem confined to the xz -plane, assuming that all fundamental variables remain independent of the y -axis. As a result, the temperature variations and displacement components are described as follows

$$v_1 = v_3 = 0, \quad \text{and} \quad v_2 = v_2(x, z, t), \quad \theta = \theta(x, z, t) \quad (6)$$

Substituting equations (4)-(6) into equation (2)-(3) transforms it into the following form

$$\rho_1 \frac{\partial^2 v_2}{\partial t^2} = \mu_1 \left(\frac{\partial^2}{\partial x^2} + \frac{\partial^2}{\partial z^2} \right) v_2, \quad (7)$$

$$K \left(\frac{\partial^2}{\partial x^2} + \frac{\partial^2}{\partial z^2} \right) \theta - c_v \frac{\partial \theta}{\partial t} = 0, \quad (8)$$

where $c_v = aT_0$ represents an effective thermal parameter associated with thermal relaxation.

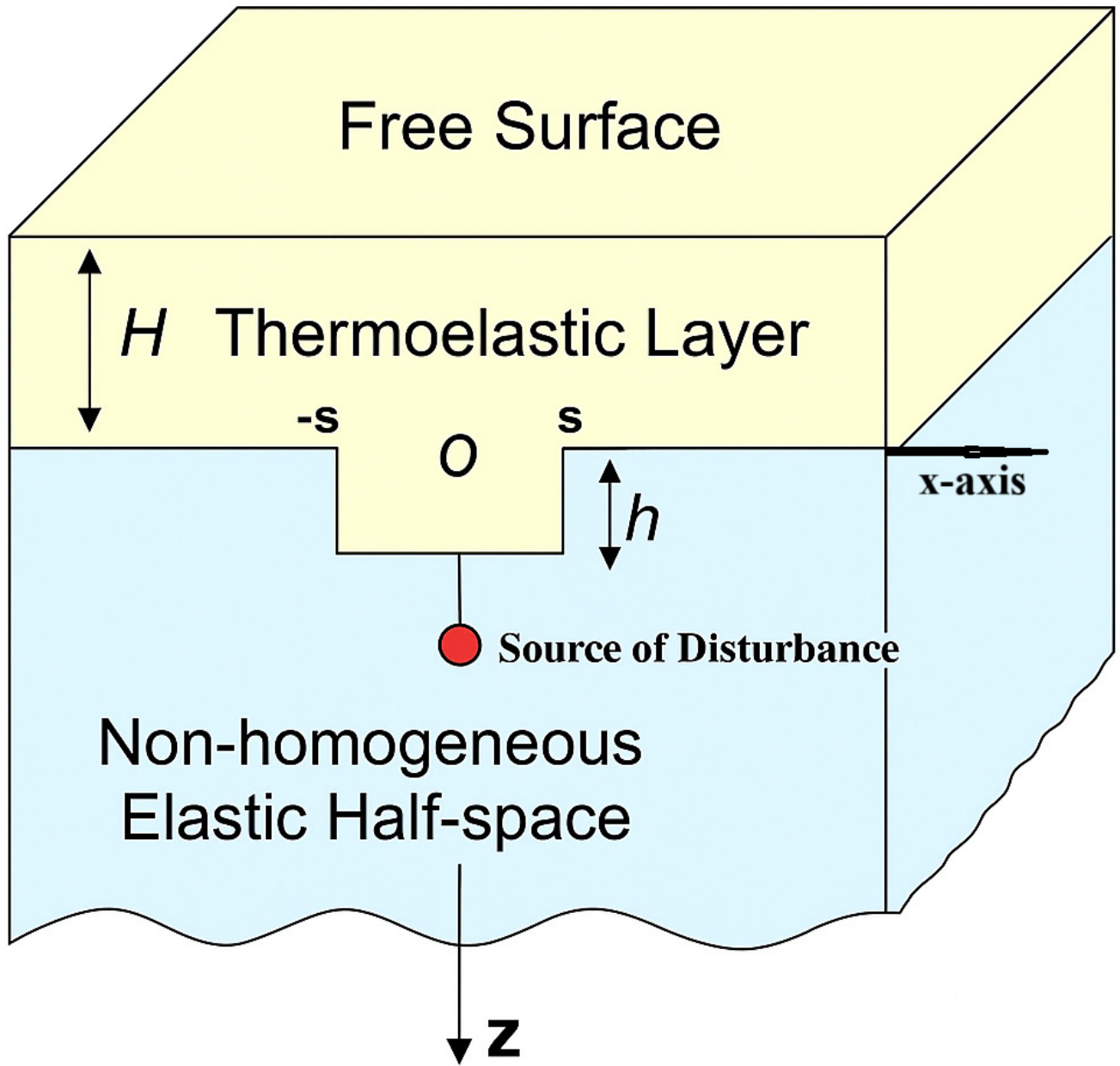


Figure 1. Geometry of considered problem.

As outlined in the theory proposed by Konczak [25], the fundamental equations and material relations for medium M_2 , assuming no body forces or external heat sources are present, can be represented as follows

$$\sigma_{ij,j} = \rho_2 \dot{w}_i, \tag{9}$$

where σ_{ij} and ρ_2 represents the stress tensor component and density, respectively.

The constitutive relation for the medium M_2 can be written

as follows

$$\sigma_{ij} = \lambda_2 p_{kk} \delta_{ij} + 2\mu_2 p_{ij}, \tag{10}$$

where

$$p_{ij} = \frac{1}{2}(w_{i,j} + w_{j,i}), \quad p_{kk} = w_{kk}. \tag{11}$$

Equation (9) by using equations (10)-(11) with considera-

tion $w_1 = w_3 = 0$, and $w_2 = w_2(x, z, t)$ changes to

$$\left\{ \frac{\partial^2}{\partial x^2} + \frac{\partial^2}{\partial z^2} \right\} w_2 + \frac{1}{\mu_2} \frac{d\mu_2}{dz} \frac{\partial w_2}{\partial z} = \frac{1}{c_2^2} \frac{\partial^2 w_2}{\partial t^2}, \quad (12)$$

where $c_2^2 = \frac{\mu_2}{\rho_2}$, denotes the shear wave velocity in the half-space.

The shear elastic modulus μ_2 and mass density ρ_2 of half-space are assumed to vary exponentially with depth as

$$\rho_2 = \rho_0 \exp(qz), \quad \mu_2 = \mu_0 \exp(qz), \quad (13)$$

where μ_0 , and ρ_0 are reference values, and q is the inhomogeneity parameter with dimensions of inverse length (m^{-1}), ensuring dimensional consistency of the exponential variation of material properties.

4. Boundary conditions

Two types of boundary conditions are taken into account in the analysis. One applied to the upper surface of the layer and the other at the interface separating medium M_1 and the medium M_2 :

4.1. Mechanical boundary conditions:

The upper surface of the thermoelastic layer is considered free from any external mechanical stress. At the contact between the thermoelastic layer and the nonhomogeneous elastic half-space, the two media are considered to be perfectly bonded, meaning there is no slipping or separation at the interface. Under these assumptions, the mechanical boundary conditions can be stated as follows

1. The component of stress is considered zero at $z = -H$ (free surface of the layer). i.e.

$$t_{32} = 0. \quad (14)$$

2. The component of displacement remains continuous across the interface $z = \varepsilon f(x)$ i.e.

$$v_2(x, z = \varepsilon f(x), t) = w_2(x, z = \varepsilon f(x), t). \quad (15)$$

3. The stress components at the interface between medium M_1 and medium M_2 are taken to be continuous. i.e.

$$t_{32} = \sigma_{32}, \quad (16)$$

Accounting for the non-planar geometry of the interface and using the stress-strain relations, this condition takes the form

$$\mu_1 \left(\frac{\partial v_2}{\partial z} - \varepsilon f'(x) \frac{\partial v_2}{\partial x} \right) = \mu_0 \left(\frac{\partial w_2}{\partial z} - \varepsilon f'(x) \frac{\partial w_2}{\partial x} \right). \quad (17)$$

Additionally, the second term on both sides of equation (17) appears due to the irregularity present at the interface.

4.2. Thermal boundary conditions:

This study considers thermal insulation of the layer, meaning the temperature component is constant (fixed) at the upper free surface and at interface separating medium M_1 and medium M_2 .

1. At the free upper surface $z = -H$

$$\theta(x, -H, t) = 0. \quad (18)$$

2. At the interface separating medium M_1 and the medium M_2 i.e. at $z = \varepsilon f(x)$

$$\theta(x, \varepsilon f(x), t) = 0. \quad (19)$$

These conditions ensure a clear definition of stress, thermal and displacement behaviour at both the interface of contact and the free upper surface, ensuring the continuity and compatibility needed for accurate physical modelling.

5. Solution of the problem

For the waves propagating harmonically with respect to time, the fundamental variables can be expressed in a harmonic form as

$$\{v_2, w_2, \theta\}(x, z, t) = \{v_2^0, w_2^0, \theta^0\}(x, z) e^{-i\omega t}. \quad (20)$$

By applying equation (20), the motion equations for each medium previously presented in equations (7)-(8) and (12), are rewritten in the following form:

$$\left\{ \frac{\partial^2}{\partial x^2} + \frac{\partial^2}{\partial z^2} + \frac{\omega^2}{c_t^2} \right\} v_2^0 = 0, \quad (21)$$

$$\left\{ K \left(\frac{\partial^2}{\partial x^2} + \frac{\partial^2}{\partial z^2} \right) + i\omega c_v \right\} \theta^0 = 0, \quad (22)$$

$$\left\{ \frac{\partial^2}{\partial z^2} + q \frac{\partial}{\partial z} - k^2 \left(1 - \frac{c_L^2}{c_0^2} \right) \right\} w_2^0 = 0, \quad (23)$$

where $\omega = kc_L$, $c_t = \sqrt{\mu_1/\rho_1}$, and $c_0 = \sqrt{\mu_0/\rho_0}$.

The Fourier transform of $u_2^0(x, z)$, along with its inverse transform, is given by the following expressions.

$$\overline{u_2^0}(\eta, z) = \int_{-\infty}^{\infty} u_2^0(x, z) e^{i\eta x} dx, \quad (24)$$

$$u_2^0(x, z) = \frac{1}{2\pi} \int_{-\infty}^{\infty} \overline{u_2^0}(\eta, z) e^{-i\eta x} d\eta. \quad (25)$$

Using equation (24) into equations (21)-(23) results a corresponding system of differential equations.

$$\frac{d^2 \overline{v_2^0}}{dz^2} + \Psi_1^2 \overline{v_2^0} = 0, \quad (26)$$

$$\frac{d^2 \overline{\theta^0}}{dz^2} + \Psi_2^2 \overline{\theta^0} = 0, \quad (27)$$

$$\frac{d^2 \overline{w_2^0}}{dz^2} + q \frac{d\overline{w_2^0}}{dz} - \Psi^2 \overline{w_2^0} = 0, \quad (28)$$

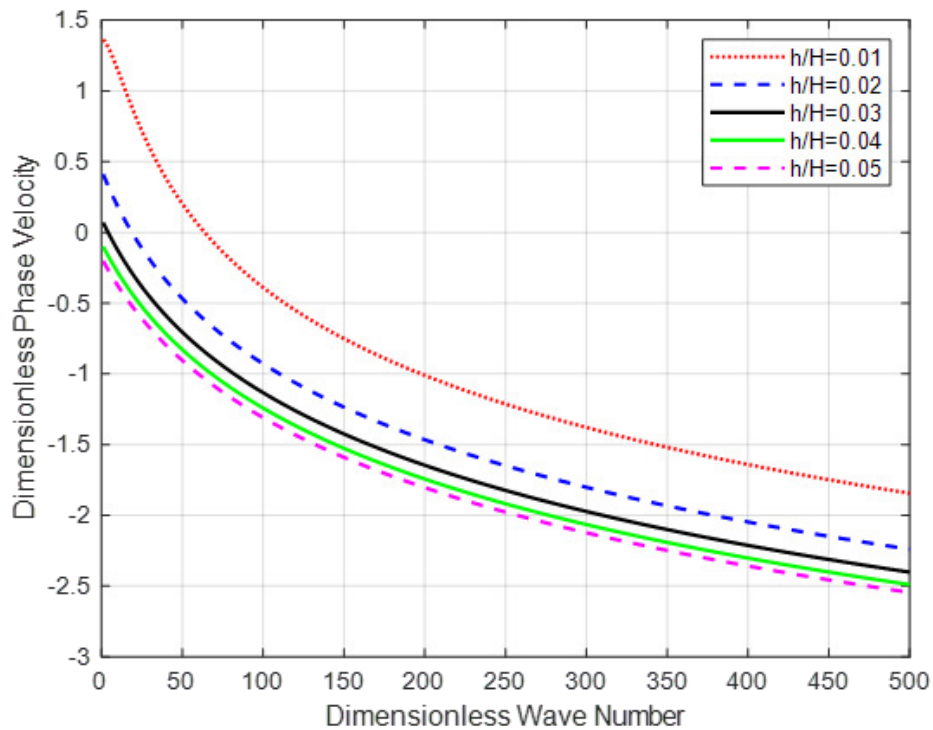


Figure 2. This figure presents the relationship between the dimensionless phase velocity and the dimensionless wave number when the inhomogeneity parameter is set to $q = 0$.

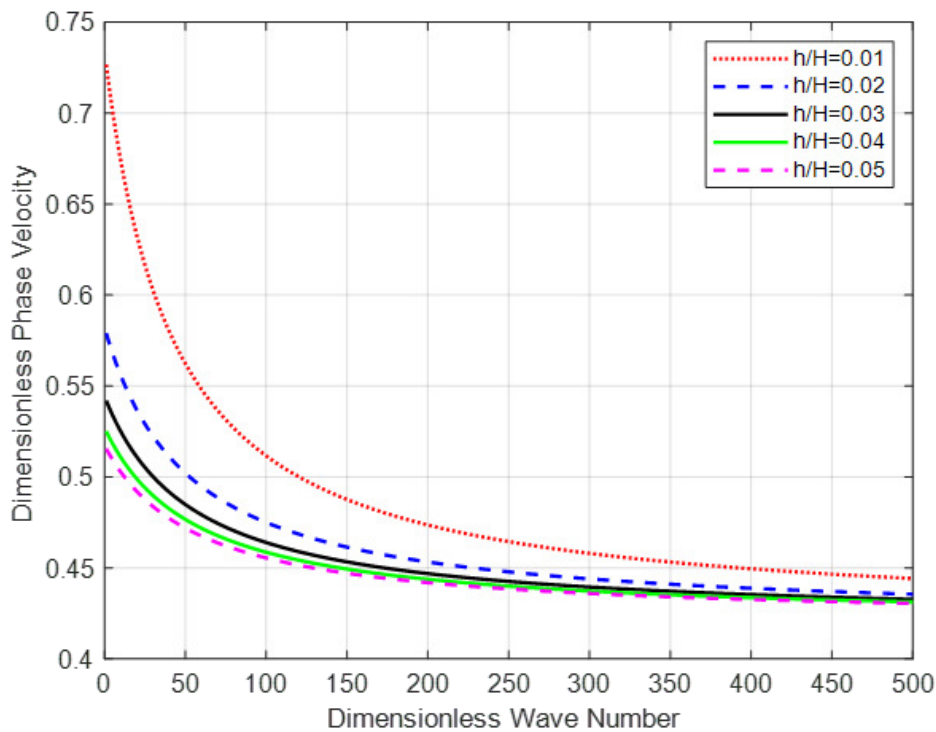


Figure 3. This figure presents the relationship between the dimensionless phase velocity and the dimensionless wave number when the inhomogeneity parameter is set to $q = 1$.

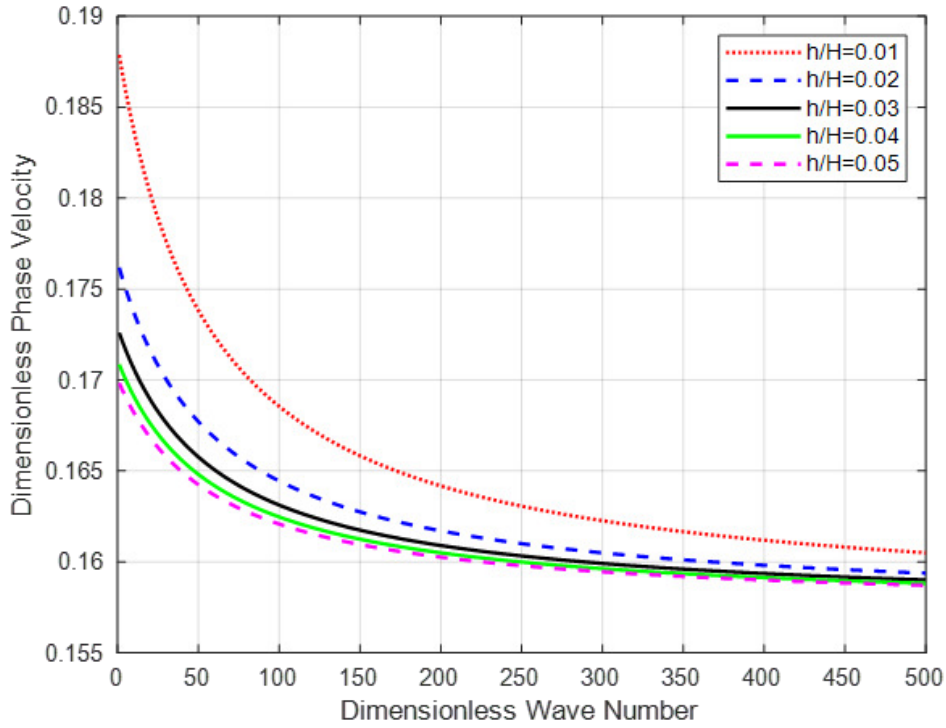


Figure 4. This figure presents the relationship between the dimensionless phase velocity and the dimensionless wave number when the inhomogeneity parameter is set to $q = 2$.

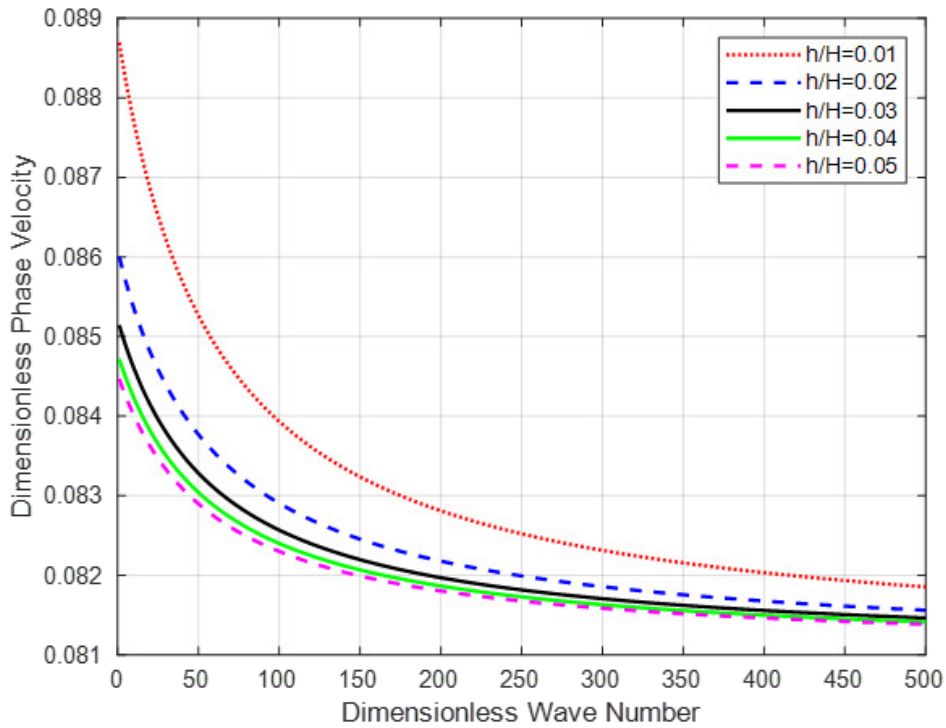


Figure 5. This figure presents the relationship between the dimensionless phase velocity and the dimensionless wave number when the inhomogeneity parameter is set to $q = 3$.

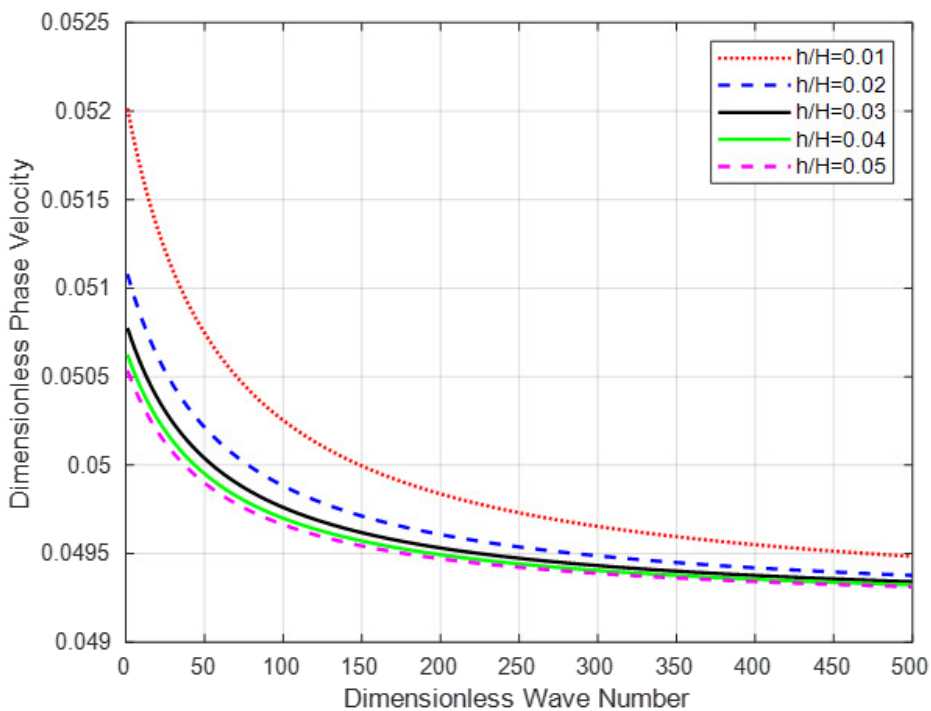


Figure 6. This figure presents the relationship between the dimensionless phase velocity and the dimensionless wave number when the inhomogeneity parameter is set to $q = 4$.

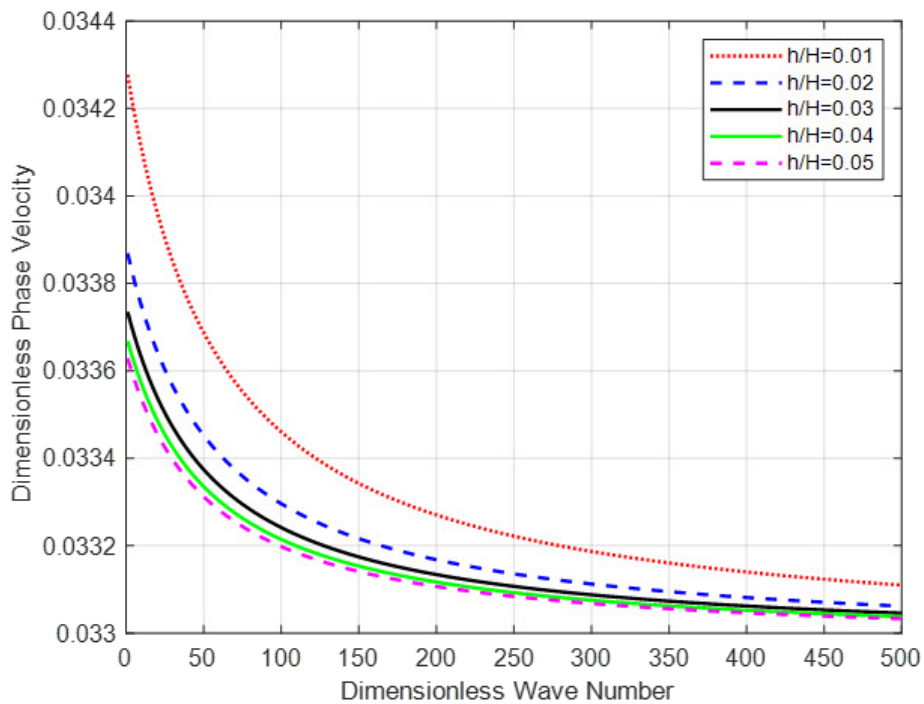


Figure 7. This figure presents the relationship between the dimensionless phase velocity and the dimensionless wave number when the inhomogeneity parameter is set to $q = 5$.

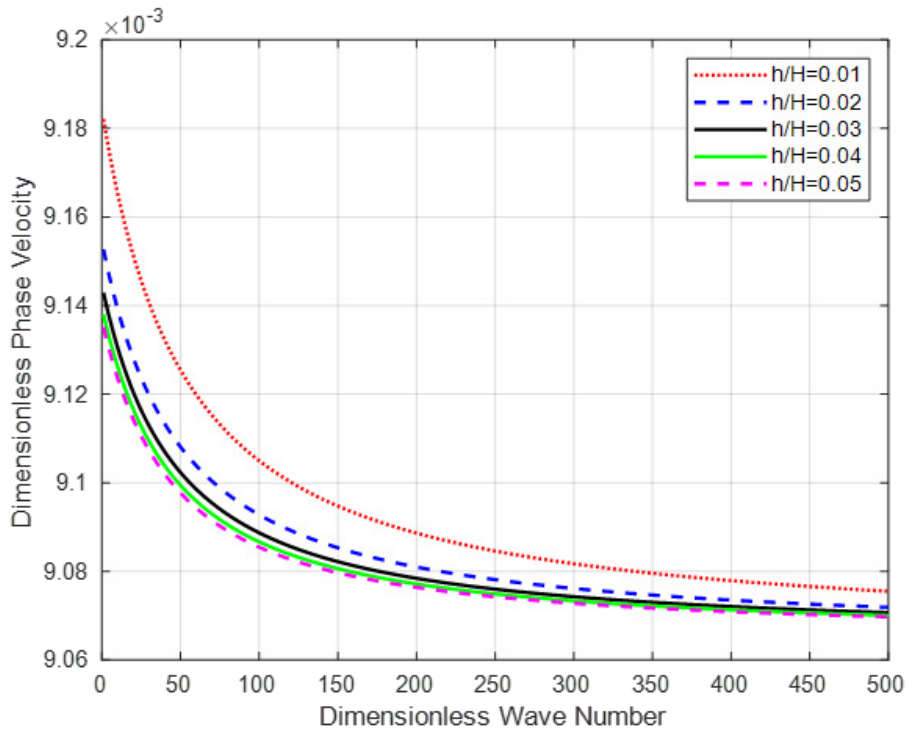


Figure 8. This figure presents the relationship between the dimensionless phase velocity and the dimensionless wave number when the inhomogeneity parameter is set to $q = 10$.

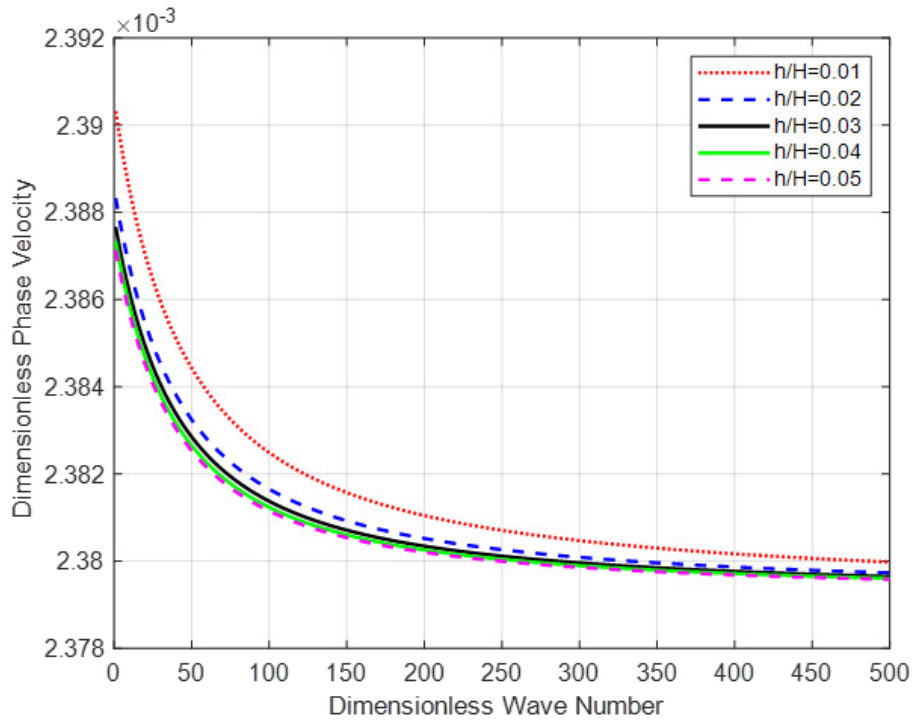


Figure 9. This figure presents the relationship between the dimensionless phase velocity and the dimensionless wave number when the inhomogeneity parameter is set to $q = 20$.

where Ψ_1^2 , Ψ_2^2 and Ψ^2 are defined as

$$\Psi_1^2 = \left(-\eta^2 + \frac{\omega^2}{c_T^2}\right), \Psi_2^2 = -\eta^2 - \frac{i\omega c_V}{K}, \Psi^2 = \eta^2 - \frac{\omega^2}{c_0^2}. \quad (29)$$

The general form of the solution to the differential equations given in equations (26)-(28) can be written as follows

$$\bar{v}_2^0 = A_1 \cos(\Psi_1 z) + A_2 \sin(\Psi_1 z), \tag{30}$$

$$\bar{\theta}^0 = A_3 \cos(\Psi_2 z) + A_4 \sin(\Psi_2 z), \tag{31}$$

$$\bar{w}_2^0 = A_5 \exp(-\Psi_3 z), \tag{32}$$

where A_1, A_2, \dots, A_5 are arbitrary functions of η and $\Psi_3 = \frac{1}{2}(q + \sqrt{q^2 + 4\Psi^2})$.

Applying the inverse Fourier transformation from equation (25), equations (30) to (32) are modified as follows

$$v_2^0(x, z) = \frac{1}{2\pi} \int_{-\infty}^{\infty} (A_1 \cos(\Psi_1 z) + A_2 \sin(\Psi_1 z)) e^{-i\eta x} d\eta, \tag{33}$$

$$\theta^0(x, z) = \frac{1}{2\pi} \int_{-\infty}^{\infty} (A_3 \cos(\Psi_2 z) + A_4 \sin(\Psi_2 z)) e^{-i\eta x} d\eta, \tag{34}$$

$$w_2^0(x, z) = \frac{1}{2\pi} \int_{-\infty}^{\infty} \left(A_5 e^{-\Psi_3 z} + \frac{2}{\Psi_3} e^{-\Psi_3 z} e^{-\Psi_3 d} \right) e^{-i\eta x} d\eta, \tag{35}$$

The second term in the integrand in equation (35) is due the presence of the source of disturbance at a distance d from the origin on the z -axis in the half-space.

6. Methodology for solution of the problem

The perturbation technique [36] is employed to effectively manage the mathematical complexity introduced by the rectangular-shaped interface irregularity and the associated boundary conditions. A dimensionless parameter ε is introduced, allowing the solution to be approximated in a controlled way.

The arbitrary functions A_1, A_2, \dots, A_5 can be expressed for very small constant ε as

$$A_1 \equiv A_1^0 + A_1^1 \varepsilon, \quad A_2 \equiv A_2^0 + A_2^1 \varepsilon, \tag{36}$$

$$A_3 \equiv A_3^0 + A_3^1 \varepsilon, \quad A_4 \equiv A_4^0 + A_4^1 \varepsilon, \tag{37}$$

$$A_5 \equiv A_5^0 + A_5^1 \varepsilon, \tag{38}$$

$$e^{\pm \alpha \varepsilon f} \cong 1 \pm \alpha \varepsilon f, \tag{39}$$

$$\sin(\Psi_1 \varepsilon f) \cong \Psi_1 \varepsilon f, \quad \cos(\Psi_1 \varepsilon f) \cong 1. \tag{40}$$

By using boundary conditions at $z = -H$, and substituting the equations (36)-(40) into equations (33)-(35), following expressions are obtained.

$$(A_1^0 + A_1^1 \varepsilon) \cos(\Psi_1 H) + (A_2^0 + A_2^1 \varepsilon) \sin(\Psi_1 H) = 0, \tag{41}$$

$$(A_3^0 + A_3^1 \varepsilon) \cos(\Psi_2 H) - (A_4^0 + A_4^1 \varepsilon) \sin(\Psi_2 H) = T_0. \tag{42}$$

By using boundary conditions at $z = \varepsilon f(x)$, and substituting the equations (36) to (40) into equations (33) to (35), following expressions are obtained.

$$(A_3^0 + A_3^1 \varepsilon) \cos(\Psi_2 \varepsilon f(x)) + (A_4^0 + A_4^1 \varepsilon) \sin(\Psi_2 \varepsilon f(x)) = T_0, \tag{43}$$

$$\begin{aligned} & \int_{-\infty}^{\infty} \left((A_1^0 + A_1^1 \varepsilon) \cos(\Psi_1 \varepsilon f(x)) + (A_2^0 + A_2^1 \varepsilon) \sin(\Psi_1 \varepsilon f(x)) \right) e^{-i\eta x} d\eta \\ &= \int_{-\infty}^{\infty} \left((A_3^0 + A_3^1 \varepsilon) e^{-\Psi_3 \varepsilon f(x)} + \frac{2}{\Psi_3} e^{-\Psi_3 \varepsilon f(x)} e^{-\Psi_3 d} \right) e^{-i\eta x} d\eta, \end{aligned} \tag{44}$$

$$\begin{aligned} & \int_{-\infty}^{\infty} \left[- (A_1^0 + A_1^1 \varepsilon) \sin(\Psi_1 \varepsilon f(x)) + (A_2^0 + A_2^1 \varepsilon) \cos(\Psi_1 \varepsilon f(x)) \right. \\ & \quad \left. - \varepsilon f'(x) ((A_1^0 + A_1^1 \varepsilon) \cos(\Psi_1 \varepsilon f(x)) \right. \\ & \quad \left. + (A_2^0 + A_2^1 \varepsilon) \sin(\Psi_1 \varepsilon f(x))) \right] e^{-i\eta x} d\eta \\ &= \int_{-\infty}^{\infty} \left[- \Psi_3 (A_3^0 + A_3^1 \varepsilon) e^{-\Psi_3 \varepsilon f(x)} - 2 e^{-\Psi_3 \varepsilon f(x)} e^{-\Psi_3 d} \right. \\ & \quad \left. - \eta (A_3^0 + A_3^1 \varepsilon) e^{-\Psi_3 \varepsilon f(x)} - \frac{2}{\Psi_3} \eta e^{-\Psi_3 \varepsilon f(x)} e^{-\Psi_3 d} \right] e^{-i\eta x} d\eta. \end{aligned} \tag{45}$$

The Fourier transform and its inverse transform for $f(x)$ in equation (1) are

$$\bar{f}(\lambda) = \int_{-\infty}^{\infty} f(x) e^{i\lambda x} dx, \tag{46}$$

$$f(x) = \frac{1}{2\pi} \int_{-\infty}^{\infty} \bar{f}(\lambda) e^{-i\lambda x} d\lambda, \tag{47}$$

Therefore,

$$f'(x) = \frac{-i}{2\pi} \int_{-\infty}^{\infty} \lambda \bar{f}(\lambda) e^{-i\lambda x} d\lambda. \tag{48}$$

The equations (43) to (45) can be simplified by applying the equations (46) to (48) and perturbation approximation

$$(A_3^0 + A_3^1 \varepsilon) + (A_4^0 + A_4^1 \varepsilon) \Psi_2 \varepsilon f(x) = T_0, \tag{49}$$

$$\begin{aligned} & \int_{-\infty}^{\infty} \left(A_1^0 + A_1^1 \varepsilon + (A_2^0 + A_2^1 \varepsilon) \Psi_1 \varepsilon f(x) \right) e^{-i\eta x} d\eta = \\ & \int_{-\infty}^{\infty} \left[(A_3^0 + A_3^1 \varepsilon) (1 - \Psi_3 \varepsilon f(x)) + \frac{2}{\Psi_3} (1 - \Psi_3 \varepsilon f(x)) e^{-\Psi_3 d} \right] e^{-i\eta x} d\eta, \end{aligned} \tag{50}$$

$$\begin{aligned} & (A_1^0 - A_5^0) + \varepsilon (A_1^1 - A_5^1) - \frac{2}{\Psi_3} e^{-\Psi_3 d} = \\ & - (A_5^0 + A_5^1 \varepsilon) \Psi_3 \varepsilon f(x) - (A_2^0 + A_2^1 \varepsilon) \Psi_1 \varepsilon f(x) - 2 \varepsilon f(x) e^{-\Psi_3 d}, \end{aligned} \tag{51}$$

$$\left(A_1^0 - A_5^0 - \frac{2}{\Psi_3} e^{-\Psi_3 d} \right) + \varepsilon (A_1^1 - A_5^1) = \varepsilon R_1, \tag{52}$$

$$\begin{aligned} & \mu_1 \left[- (A_1^0 + A_1^1 \varepsilon) \Psi_1 \varepsilon f(x) + (A_2^0 + A_2^1 \varepsilon) \right. \\ & \quad \left. - \varepsilon f'(x) ((A_1^0 + A_1^1 \varepsilon) + (A_2^0 + A_2^1 \varepsilon) \Psi_1 \varepsilon f(x)) \right] \end{aligned}$$

Table 1. Numerical values of the physical parameters.

Parameters	Numerical Values
λ_1	1.5×10^{10} Pa
λ_2	1.3×10^{10} Pa
μ_1	7.5×10^9 N/m ²
μ_0	7.84×10^9 N/m ²
ρ_1	2100 kg/m ³
ρ_0	5563 kg/m ³
T_0	373 K
K	1.5×10^2 W m ⁻¹ K ⁻¹

$$= \mu_0 [-\Psi_3(A_5^0 + A_5^1 \varepsilon)(1 - \Psi_3 \varepsilon f(x)) - 2(1 - \Psi_3 \varepsilon f(x))e^{-\Psi_3 d} - \eta(A_5^0 + A_5^1 \varepsilon)(1 - \Psi_3 \varepsilon f(x)) - \frac{2}{\Psi_3} \eta(1 - \Psi_3 \varepsilon f(x))e^{-\Psi_3 d}], \quad (53)$$

$$\begin{aligned} & \mu_1(A_2^0 + A_2^1 \varepsilon) + \mu_0 \Psi_3(A_5^0 + A_5^1 \varepsilon) + 2\mu_0 e^{-\Psi_3 d} \\ & + \eta \mu_0(A_5^0 + A_5^1 \varepsilon) + \frac{2}{\Psi_3} \mu_0 \eta e^{-\Psi_3 d} = \\ & (A_1^0 + A_1^1 \varepsilon) \mu_1 \Psi_1 \varepsilon f(x) + \varepsilon \mu_1 f'(x) (A_1^0 + A_1^1 \varepsilon) \\ & + (A_2^0 + A_2^1 \varepsilon) \Psi_1 \varepsilon f(x) + \mu_0 \Psi_3^2 (A_5^0 + A_5^1 \varepsilon) \varepsilon f(x) + 2\mu_0 \Psi_3 \varepsilon f(x) e^{-\Psi_3 d} \\ & + \eta \mu_2 (A_5^0 + A_5^1 \varepsilon) f(x) + 2\varepsilon \Psi_3 e^{-\Psi_3 d} f(x), \quad (54) \end{aligned}$$

$$\begin{aligned} & \left(\mu_1 A_2^0 + \mu_0 \Psi_3 A_5^0 + \eta \mu_0 A_5^0 + 2\mu_0 e^{-\Psi_3 d} + \frac{2}{\Psi_3} \mu_0 \eta e^{-\Psi_3 d} \right) \\ & + \varepsilon \left(\mu_1 A_2^1 + \mu_0 \Psi_3 A_5^1 + \eta \mu_0 A_5^1 \right) = \varepsilon R_2, \quad (55) \end{aligned}$$

where

$$R_1(k) = \frac{1}{2\pi} \int_{-\infty}^{\infty} (-A_5^0 \Psi_3 - A_2^0 \Psi_1 - 2e^{-\Psi_3 d}) \bar{f}(\lambda) d\lambda, \quad (56)$$

$$\begin{aligned} R_2(k) = \frac{1}{2\pi} \int_{-\infty}^{\infty} & \left(A_1^0 \mu_1 \Psi_1 + \mu_0 \Psi_3 (\Psi_3 A_5^0 + 2e^{-\Psi_3 d}) \right. \\ & \left. + \mu_0 \lambda k (\Psi_3 A_5^0 - 2e^{-\Psi_3 d}) \right) \bar{f}(\lambda) d\lambda. \quad (57) \end{aligned}$$

Now, by separating equations (41)-(42) and (49)-(55) into terms that contains ε and those independent of ε , we obtained a system of ten nonhomogeneous linear equations in the unknowns $A_1^0, A_2^0, \dots, A_5^0, A_1^1, A_2^1, \dots, A_5^1$.

$$A_1^0 \cos(\Psi_1 H) + A_2^0 \sin(\Psi_1 H) = 0, \quad (58)$$

$$A_1^1 \cos(\Psi_1 H) + A_2^1 \sin(\Psi_1 H) = 0, \quad (59)$$

$$A_3^0 \cos(\Psi_2 H) - A_4^0 \sin(\Psi_2 H) = T_0, \quad (60)$$

$$A_3^1 \cos(\Psi_2 H) - A_4^1 \sin(\Psi_2 H) = 0, \quad (61)$$

$$A_3^0 + A_4^0 \Psi_2 \varepsilon f(x) = T_0, \quad (62)$$

$$A_3^1 + A_4^1 \Psi_2 \varepsilon f(x) = 0, \quad (63)$$

$$A_1^0 - A_5^0 = \frac{2}{\Psi_3} e^{-\Psi_3 d}, \quad (64)$$

$$A_1^1 - A_5^1 = R_1, \quad (65)$$

$$\mu_1 A_2^0 + \eta \mu_0 A_5^0 = 2\mu_0 e^{-\Psi_3 d} - \frac{2}{\Psi_3} \mu_0 \eta e^{-\Psi_3 d}, \quad (66)$$

$$\mu_1 A_2^1 + \eta \mu_0 A_5^1 = R_2. \quad (67)$$

By solving this system of equations, the corresponding unknown parameters can be determined.

$$A_1^0 = -\frac{2\mu_0 \tan(\Psi_1 H) e^{-\Psi_3 d}}{E} \quad (68)$$

$$A_2^0 = \frac{2\mu_0 e^{-\Psi_3 d}}{E} \quad (69)$$

$$A_3^0 = T_0 \quad (70)$$

$$A_4^0 = T_0 (\cot(\Psi_2 H) - \csc(\Psi_2 H)) \quad (71)$$

$$A_5^0 = -\frac{2e^{-\Psi_3 d} (\Psi_3 \mu_0 \tan(\Psi_1 H) + E)}{E \Psi_3} \quad (72)$$

$$A_1^1 = -\frac{(R_2 + \mu_0 \Psi_3 R_1) \tan(\Psi_1 H)}{E} \quad (73)$$

$$A_2^1 = \frac{R_2 + \mu_0 \Psi_3 R_1}{E} \quad (74)$$

$$A_3^1 = A_4^1 = 0 \quad (75)$$

$$A_5^1 = -\frac{(R_2 + \Psi_3 \mu_0 R_1) \tan(\Psi_1 H) + R_1 E}{E} \quad (76)$$

where

$$E = \mu_1 \Psi_1 - \mu_0 \Psi_3 \tan(\Psi_1 H). \quad (77)$$

Substituting these values into equations (33)-(35), the expression for the temperature variable and displacement vector are obtained as follows

$$\begin{aligned} v_2^0 = \frac{1}{2\pi} \int_{-\infty}^{\infty} & \left[\frac{2e^{-\Psi_3 d} \mu_0}{E} \left(1 + \frac{\varepsilon (R_2 + \mu_0 \Psi_3 R_1) e^{\Psi_3 d}}{2\mu_0} \right) \sin(\Psi_1 z) \right. \\ & \left. + \tan(\Psi_1 H) \cos(\Psi_1 z) \right] e^{-ikx} dk, \quad (78) \end{aligned}$$

$$\begin{aligned} \theta^0(x, z) = \frac{1}{2\pi} \int_{-\infty}^{\infty} & \left[\frac{T_0}{\sin(\Psi_2 H)} (\sin(\Psi_2 H + \Psi_2 z) \right. \\ & \left. - \sin(\Psi_2 z)) \right] e^{-inx} d\eta. \quad (79) \end{aligned}$$

Using the equation of rectangular-shaped interface irregularity (equation (1)) and its Fourier transformation,

$$\bar{h}(\lambda) = \frac{4s}{\lambda} \sin(\lambda s). \quad (80)$$

Using equations (56) and (57) along with equation (80), the expression $R_2 + \mu_0 \eta R_1$ simplifies to:

$$R_2 + \mu_0 \Psi_3 R_1 = \frac{4s\mu_0}{\pi} \int_0^{\infty} [g(k - \lambda) + g(k + \lambda)] \frac{\sin(\lambda s)}{\lambda} d\lambda. \quad (81)$$

Now, by applying the asymptotic formula provided by Willis [37], the integral in equation (81) simplifies to

$$R_2 + \mu_0 \Psi_3 R_1 = \frac{4s\mu_0}{\pi} \left(\frac{\pi}{2} \cdot 2g(k) \right). \quad (82)$$

By using equation of rectangular-shaped interface irregularity, the equation can be simplified as

$$R_2 + \mu_0 \Psi_3 R_1 = \frac{2h\mu_0 g(k)}{\varepsilon}, \quad (83)$$

where

$$g(k - \lambda) = \left[A_1^0 \mu_1 \Psi_1 + \Psi_3^2 A_5^0 + 2\Psi_3 e^{-\Psi_3 d} - \mu_0 \lambda k (A_5^0 \Psi_3 - A_2^0 \Psi_1 - 2e^{-\Psi_3 d}) \right]. \quad (84)$$

From equation (83), the component of displacement in M_1 changes to

$$v_2^0 = \frac{1}{2\pi} \int_{-\infty}^{\infty} \left(\frac{2e^{-\Psi_3 d} \mu_0}{E} [1 + hg(k)e^{\Psi_3 d}] \times [\sin(\Psi_1 z) + \tan(\Psi_1 H) \cos(\Psi_1 z)] e^{-ikx} \right) dk. \quad (85)$$

The integral in equation (85) mainly depends on the poles of integrand, so the dispersion relation is obtained by identifying the roots of the corresponding equation

$$E [1 - hg(k)e^{\Psi_3 d}] = 0. \quad (86)$$

The dispersion relation for the Love-type surface waves is obtained.

$$\tan(\Psi_1 H) = \frac{2h(2\Psi_3 \mu_1 - 2\mu_1 k - \Psi_1 \mu_0) - \mu_1 \Psi_1}{2h\Psi_3(\Psi_3 \mu_0 k - \mu_0) - 2h(\Psi_1 \mu_1 - 2\mu_0 k) - \mu_0 \Psi_3}. \quad (87)$$

Considering the following terms for simplification

$$\Psi_1 = P_1 k, \quad \Psi_3 = P_3 k, \quad q = Qk, \quad (88)$$

$$\Psi_1^2 = \left(-\eta^2 + \frac{\omega^2}{c_t^2} \right) = \left(\frac{c_L^2}{c_t^2} - 1 \right) k^2, \quad (89)$$

$$P_1 = \sqrt{\frac{c_L^2}{c_t^2} - 1}, \quad (90)$$

$$\Psi_3 = \frac{1}{2} \left(Qk + k \sqrt{Q + 4 \left(1 - \frac{c_L^2}{c_0^2} \right)} \right), \quad (91)$$

$$P_3 = \frac{1}{2} \left(Q + \sqrt{Q + 4 \left(1 - \frac{c_L^2}{c_0^2} \right)} \right), \quad (92)$$

where Q is a dimensionless inhomogeneity parameter and k denotes the wave number.

By substituting these values, the final form of dispersion relation for the Love waves becomes

$$\tan(P_1 k H) = \frac{2kh(2P_3 \mu_1 - 2\mu_1 - P_1 \mu_0) - \mu_1 P_1 k}{2hP_3 k(P_3 \mu_0 k - \mu_0) - 2hk(P_1 \mu_1 - 2\mu_0) - \mu_0 P_3 k}. \quad (93)$$

Special Case: For the configuration where the interface irregularity is removed by setting $h = 0$ in equation (87). It is simplified to

$$\tan(\Psi_1 H) = \frac{\mu_1 \Psi_1}{\mu_0 \Psi_3}. \quad (94)$$

This equation corresponds to the classical dispersion relation for Love waves.

7. Numerical analysis and discussions

The numerical analysis of Love wave propagation in an isotropic thermoelastic layer with a free upper surface over a nonhomogeneous elastic half-space is carried out using MATLAB. Graphical results are used to study how different physical parameters influence wave behaviour. The mechanical and thermal properties of the upper layer are selected following the work of Kumar *et al.* [23], while the elastic parameters for the nonhomogeneous half-space are adopted from Gubbins [2]. The chosen parameter values are listed in Table 1. These selections ensure agreement with established literature and provide a realistic foundation for examining how thermoelastic effects, rectangular interface irregularities, and material inhomogeneity affect phase velocity and dispersion characteristics.

The graphical results presented in the Figures 2-9 illustrate the dependence of the dimensionless phase velocity on the dimensionless wave number for the different values of the material inhomogeneity. The dispersive nature of the Love-type surface waves is clearly observed throughout the considered range of material parameters. The physical mechanisms responsible for these type of variations are discussed below.

At the lower wave numbers, the propagating disturbance penetrates deeper into the half-space, and therefore the wave becomes more sensitive to the spatial variation of material properties. When the inhomogeneity parameter increases, the elastic rigidity of the lower medium changes more rapidly, resulting in a reduction in the phase velocity. Hence, the stronger material inhomogeneity produces slower propagation in the long-wavelength regime.

As the wave number increases, the penetration depth of the surface wave decreases and the motion becomes increasingly confined to the upper thermoelastic layer. Consequently, the influence of the lower heterogeneous half-space diminishes. This explains why the dispersion curves corresponding to the different material inhomogeneity parameters gradually converging to each other at higher wave numbers.

Another important observation is the presence of the rectangular-shaped interface irregularity introduces additional scattering and the mode conversion effects. The geometric discontinuity alters the continuity of stress transmission across the interface. This contributes to further reduction in phase velocity.

8. Conclusion

This study examines the behaviour of Love waves in an isotropic thermoelastic layer with a free upper surface posi-

tioned above a heterogeneous half-space with a rectangular interface irregularity. The dispersion relation for this configuration has been obtained using elasticity theory along with perturbation method and Fourier transformations. The dispersion behavior is influenced by several variables, the inhomogeneity factor, the wave number, the geometry of the irregularity, and the layer thickness. The numerical calculations with graphical analysis help to understand clearly how these parameters affect the dimensionless phase velocity in comparison to the dimensionless wave number. The main findings of analytical and numerical studies are given as follows:

- Effect of inhomogeneity: An increase in inhomogeneity parameter (q) leads to a decrease in phase velocity with respect to wave number, indicating that stronger the inhomogeneity of the lower half-space, larger the dispersive effects and slows down Love wave propagation in this configuration.
- Effect of irregularity depth to layer's height ratio (h/H): Increasing the depth of the rectangular irregularity (larger h/H) generally reduces the phase velocity (for fixed q). This shows that deeper irregularities enhance scattering and increase dispersion, producing slower effective surface propagation.
- Combined parameter effects: The slowest phase velocities are observed when both q and h/H are large: inhomogeneity and deep irregularity act together to maximize dispersion and attenuation. Conversely, the least dispersive behaviour occurs for small q and shallow irregularity.

These findings provide a better understanding of the seismic wave propagation behaviour in the thermoelastic, nonhomogeneous and irregular media, which have high degree of application in material science, geophysics and structural engineering. Thermoelastic effects influences attenuation and dispersion primarily at higher frequencies. Its net effect on phase velocity is smaller than that of material inhomogeneity and interface geometry in the parameter ranges considered, but it contributes to attenuation trends visible in the numerical results. These results emphasize that neglecting either material inhomogeneity considerations or interface irregularity can lead to substantial misestimation of Love-wave speeds in layered media. These results are relevant to seismic site-response measurements, subsurface imaging, as well as development of wave-based sensing modalities in layered thermoelastic systems.

Data availability

No external datasets were used in this study. All analytical derivations and numerical results are generated within the framework of the model presented in this manuscript.

Acknowledgment

The authors acknowledge the Department of Mathematics, Chandigarh University, for providing the institutional support.

References

- [1] P. M. Shearer, *Introduction to seismology*, Cambridge University Press, Cambridge, United Kingdom, 2019. <https://www.cambridge.org/highereducation/books/introduction-to-seismology/C1471C1B553C05997E2BC7EB26D4C26D#overview>.
- [2] D. Gubbins, *Seismology and plate tectonics*, Cambridge University Press, Cambridge, United Kingdom, 1990.
- [3] M. A. Biot, *Mechanics of incremental deformations*, John Wiley & Sons, New York, USA, 1965. <https://hal.science/hal-01352219/>.
- [4] A. E. H. Love, *Some problems of geodynamics*, Cambridge University Press, Cambridge, United Kingdom, 1911. <https://ui.adsabs.harvard.edu/abs/1911spge.book.....L/abstract>.
- [5] W. M. Ewing, W. S. Jardetzky, F. Press & A. Beiser, "Elastic waves in layered media", *Physics Today* **10** (1957) 27. <https://doi.org/10.1063/1.3060163>.
- [6] K. F. Graff, *Wave motion in elastic solids*, Dover Publications, New York, USA, 1991. <https://trid.trb.org/View/59547>.
- [7] J. Achenbach, *Wave propagation in elastic solids*, North-Holland Publishing, Amsterdam, Netherlands, 2012. <https://asmedigitalcollection.asme.org/appliedmechanics/article/41/2/544/422932/Vibration-of-Shells?guestAccessKey=>.
- [8] A. Chattopadhyay & B. K. Kar, "Love waves due to a point source in an isotropic elastic medium under initial stress", *International Journal of Non-Linear Mechanics* **16** (1981) 247. <https://www.sciencedirect.com/science/article/abs/pii/002074628190038X>.
- [9] S. Kundu, A. Kumari, D. K. Pandit & S. Gupta, "Love wave propagation in heterogeneous micropolar media", *Mechanics Research Communications* **83** (2017) 6. <https://www.sciencedirect.com/science/article/abs/pii/S0093641316301471>.
- [10] R. Kumar & A. Saini, "Effect of anisotropy, inhomogeneity and porosity on love wave propagation through fluid-saturated porous layers in irregular layered media", *The European Physical Journal Plus* **139** (2024) 1137. <https://link.springer.com/article/10.1140/epjp/s13360-024-05914-5>.
- [11] A. Chattopadhyay, P. Singh, P. Kumar & A. K. Singh, "Study of love-type wave propagation in an isotropic tri layers elastic medium overlying a semi-infinite elastic medium structure", *Waves in Random and Complex Media* **28** (2018) 643. <https://www.tandfonline.com/doi/abs/10.1080/17455030.2017.1381778>.
- [12] M. A. Biot, "Thermoelasticity and irreversible thermodynamics", *Journal of Applied Physics* **27** (1956) 240. <https://pubs.aip.org/aip/jap/article-abstract/27/3/240/161089/Thermoelasticity-and-Irreversible-Thermodynamics>.
- [13] W. Nowacki, *Dynamic problems of thermoelasticity*, Springer Netherlands, Dordrecht, Netherlands, 1975. <https://asmedigitalcollection.asme.org/appliedmechanics/article/44/2/366/388589/Dynamic-Problems-of-Thermoelasticity?guestAccessKey=>.
- [14] R. S. Dhaliwal & A. Singh, *Dynamic coupled thermoelasticity*, Hindustan Publishing Corporation, New Delhi, India, 1980.
- [15] H. W. Lord & Y. Shulman, "A generalized dynamical theory of thermoelasticity", *Journal of the Mechanics and Physics of Solids* **15** (1967) 299. <https://www.sciencedirect.com/science/article/abs/pii/0022509667900245>.
- [16] A. E. Green & K. Lindsay, "Thermoelasticity", *Journal of Elasticity* **2** (1972) 1. <https://doi.org/10.1007/BF00045689>.
- [17] A. E. Green & P. Naghdi, "Thermoelasticity without energy dissipation", *Journal of Elasticity* **31** (1993) 189. <https://doi.org/10.1007/BF00044969>.
- [18] D. Y. Tzou, "The generalized lagging response in small-scale and high-rate heating", *International Journal of Heat and Mass Transfer* **38** (1995) 3231. [https://doi.org/10.1016/0017-9310\(95\)00052-B](https://doi.org/10.1016/0017-9310(95)00052-B).
- [19] J. N. Sharma, D. Singh & R. Kumar, "Generalized thermoelastic waves in homogeneous isotropic plates", *The Journal of the Acoustical Society of America* **108** (2000) 848. <https://doi.org/10.1121/1.429619>.
- [20] A. Berezovski, J. Engelbrecht & G. A. Maugin, "Thermoelastic wave propagation in inhomogeneous media", *Archive of Applied Mechanics* **70** (2000) 694. <https://doi.org/10.1007/s004190000114>.
- [21] S. Chirita, "On the rayleigh surface waves on an anisotropic homogeneous thermoelastic half space", *Acta Mechanica* **224** (2013) 657. <https://doi.org/10.1007/s00707-012-0776-z>.
- [22] A. S. Pramanik & S. Biswas, "Surface waves in nonlocal thermoelastic medium with state space approach", *Journal of Thermal Stresses* **43** (2020) 667. <https://doi.org/10.1080/01495739.2020.1725821>.

- [23] D. Kumar, D. Singh & S. K. Tomar, "Love-type waves in thermoelastic solid with double porosity structure", *Waves in Random and Complex Media* (2022) 1. <https://doi.org/10.1080/17455030.2022.2155324>.
- [24] R. Kumar & S. Sharma, "Dispersion analysis of Love-type surface waves in thermoelastic layered medium with irregular interface", *Applied Physics A* **132** (2026) 220. <https://doi.org/10.1007/s00339-026-09417-1>.
- [25] Z. Konczak, "The propagation of love waves in a fluid-saturated porous anisotropic layer", *Acta Mechanica* **79** (1989) 155. <https://doi.org/10.1007/BF01187260>.
- [26] R. Kumar, A. Saini, S. Sharma & Sunaina, *Investigating SH-wave dynamics in anisotropic media with triangular surface irregularities and initial stress influence*, IET Conference Proceedings, **2024**, No. 38, 2024, pp. 433–438. <https://doi.org/10.1049/icp.2025.0977>.
- [27] R. Kumar, S. Sharma & S. Chandel, "Impact of triangular irregularity, material heterogeneity and initial stress on the propagation of shear waves in a transversely isotropic porous layer", *International Journal of Applied Mechanics and Engineering* **30** (2025) 89. <https://doi.org/10.5944/ijame/202715>.
- [28] S. Sharma & R. Kumar, *Analyzing the role of triangular surface irregularity and initial stress on SH-wave behavior in multilayer anisotropic media*, Proceedings of the 2024 International Conference on Emerging Technologies and Innovation for Sustainability (EmergIN), India, 2024, pp. 473–478. <https://doi.org/10.1109/EmergIN63207.2024.10961042>.
- [29] A. Saini & R. Kumar, "Analysis of love waves in an initially stressed transversely isotropic porous layer over heterogeneous half space with parabolic irregularity", *Journal of Vibration Engineering & Technologies* (2024) 7373. <https://doi.org/10.1007/s42417-024-01298-z>.
- [30] A. Saini & R. Kumar, "Effect of rigidity and parabolic irregularity on love wave propagation in transversely isotropic fluid-saturated porous layer lying over a nonhomogeneous half-space", *Mechanics of Solids* **59** (2024) 1094. <https://doi.org/10.1134/S0025654424602702>.
- [31] R. Kumar & A. Saini, "Influence of parabolic irregularity, inhomogeneity, initial stress and anisotropy on love wave propagation", *Mechanics of Solids* **59** (2024) 1443. <https://doi.org/10.1134/S0025654424602854>.
- [32] S. Sharma & R. Kumar, "Love wave propagation in a homogeneous thermoelastic layer over a non-homogeneous half-space with triangular irregularity", *Mechanics of Solids* **60** (2025) 4259. <https://doi.org/10.1134/S0025654425602162>.
- [33] Pragati, R. Kumar & S. Kaushal, "Effect of a moving thermal load in a modified couple stress medium with double porosity and hyperbolic two-temperature theory", *Journal of the Nigerian Society of Physical Sciences* (2026) 2959. <https://doi.org/10.46481/jnsp.2026.2959>.
- [34] P. Thakur, M. Sethi, N. Gupta & K. Gupta, "Thermal effects in rectangular plate made of rubber, copper and glass materials", *Journal of Rubber Research* **24** (2021) 147. <https://doi.org/10.1007/s42464-020-00080-6>.
- [35] A. Saini & R. Kumar, "Love wave propagation in an isotropic thermoelastic layer with rigid boundary lying over a nonhomogeneous elastic half-space", *Mathematical Methods in the Applied Sciences* (2025) 16680. <https://doi.org/10.1002/mma.70117>.
- [36] A. C. Eringen & C. J. Samuels, "Impact and moving loads on a slightly curved elastic half space", *Journal of Applied Mechanics* **26** (1959) 491. <https://asmedigitalcollection.asme.org/appliedmechanics/article-abstract/26/4/491/1111825/Impact-and-Moving-Loads-on-a-Slightly-Curved>.
- [37] H. F. Willis, "A formula for expanding an integral as a series", *The London, Edinburgh, and Dublin Philosophical Magazine and Journal of Science* **39** (1948) 455. <https://www.tandfonline.com/doi/pdf/10.1080/14786444808521694>.

Nomenclature

M_1	Homogeneous thermoelastic layer
M_2	Nonhomogeneous half-space
$\mathbf{v} = (0, v_2, 0)$	Displacement component for M_1
$\mathbf{w} = (0, w_2, 0)$	Displacement component for M_2
$\theta = T - T_0$	Change in temperature
T_0	Reference temperature
λ, μ	Lame's constants
t	Time variable
β	Thermoelastic coupling parameter
α	Coefficient of linear thermal expansion
aT_0	Effective thermal parameter
c_t	Shear wave velocity in thermoelastic layer
c_L	Phase velocity of Love waves
a	Thermal heat capacity
K	Thermal conductivity
δ_{ij}	Kronecker delta
ρ	Mass density of the material
k	Wave number
ω	Angular velocity
d	Distance of source of irregularity (length)
$f(x)$	Interface profile function
q	Inhomogeneity parameter (m^{-1})
Q	Dimensionless inhomogeneity parameter
$2s$	Maximum width of irregularity
h	Maximum depth of irregularity
t_{ij}	Stress tensor for M_1
σ_{ij}	Stress tensor for M_2
$2e_{ij} = (u_{i,j} + u_{j,i})$	Strain tensor components
H	Height of thermoelastic layer